Developmental and Comparative Immunology 46 (2014) 413–422

Contents lists available at ScienceDirect

Developmental and Comparative Immunology

journal homepage: www.elsevier.com/locate/dci

Thymus cDNA library survey uncovers novel features of immune molecules in Chinese giant salamander *Andrias davidianus*

Rong Zhu, Zhong-Yuan Chen, Jun Wang, Jiang-Di Yuan, Xiang-Yong Liao, Jian-Fang Gui, Qi-Ya Zhang *

State Key Laboratory of Freshwater Ecology and Biotechnology, Institute of Hydrobiology, Chinese Academy of Sciences, Wuhan 430072, China

ARTICLE INFO

Article history:
Received 10 May 2014
Revised 29 May 2014
Accepted 30 May 2014
Available online 5 June 2014

Keywords:
Immune gene
Immunoglobulin
Chinese giant salamander *Andrias davidianus*
Thymus cDNA library
Ranavirus-induced

ABSTRACT

A ranavirus-induced thymus cDNA library was constructed from Chinese giant salamander, the largest extant amphibian species. Among the 137 putative immune-related genes derived from this library, these molecules received particular focus: immunoglobulin heavy chains (IgM, IgD, and IgY), IFN-inducible protein 6 (IFI6), and T cell receptor beta chain (TCRβ). Several unusual features were uncovered: IgD displays a structure pattern distinct from those described for other amphibians by having only four constant domains plus a hinge region. A unique IgY form (IgY(ΔFc)), previously undescribed in amphibians, is present in serum. Alternative splicing is observed to generate IgH diversification. IFI6 is newly-identified in amphibians, which occurs in two forms divergent in subcelluar distribution and antiviral activity. TCRβ immunoscope profile follows the typical vertebrate pattern, implying a polyclonal T cell repertoire. Collectively, the pioneering survey of ranavirus-induced thymus cDNA library from Chinese giant salamander reveals immune components and characteristics in this primitive amphibian.

1. Introduction

Amphibians have a deep and rich history as model organisms for the study of development and evolution, since they serve as an important evolutionary bridge between aquatic and terrestrial vertebrates (Vogel, 1999). More importantly, they have been, and still are widely used for comparative immunological studies (Robert and Cohen, 2011). Growing evidence has showed high degree of similarity and fundamental conservation between amphibian and mammalian immune systems (Chen and Robert, 2011; Grayfer et al., 2014; Ohta et al., 2006). Even though amphibians lack the equivalent of mammalian lymph nodes, they do have a thymus that acts as the central organ of immune system (Chen and Robert, 2011). The thymus provides a unique microenvironment for the differentiation of T lymphocytes and also possesses a small population of B cells (Lee et al., 2013; Perera et al., 2013). As such, the thymus is thought to play capital roles in both cell-mediated and humoral immunity. Until now, most knowledge about amphibian immunity has concerned the model species such as *Xenopus laevis* and the axolotl (*Ambystoma mexicanum*), whose genome or transcriptome has already been sequenced and annotated (Gilchrist et al., 2004; Putta et al., 2004). In comparison, the immune characteristics of the non-model amphibians still remain largely uncharacterized.

Chinese giant salamander, *Andrias davidianus*, is the largest extant amphibian species. It is renowned as a living fossil, since it has been in existence for more than 350 million years (Gao and Shubin, 2003). Such a key phylogenetic position makes it an invaluable model of choice for evolutionary and comparative studies of immunity. Therefore, it is of great interest to elucidate the function of immune system, particular the thymus, in this primitive species. On the other hand, there is an urgent need to understand the immune system in Chinese giant salamander, due to the fact that the population decline is dramatic resulted from emerging infectious diseases (Dong et al., 2011; Geng et al., 2011). The newly-described *Andrias davidianus* ranavirus (ADRV) is regarded as a major contributor to mass mortality events of this species (Chen et al., 2013; Chinchar and Waltzek, 2014). While the pathological process is well-characterized (Ma et al., 2014; Meng et al., 2014; Zhang and Gui, 2012), remarkably little is known about host defense against ADRV, which hampers the development of effective strategies for disease control. In this context, we sought to determine candidate genes in response to ADRV infection in

Abbreviations: IgH, immunoglobulin heavy chain gene; C_H, IgH constant region; V_H, IgH variable region; IFI6, IFN-inducible protein 6; TCRβ, T cell receptor beta chain; ADRV, *Andrias davidianus* ranavirus; CGST, Chinese giant salamander thymus cells.

* Corresponding author. Address: Institute of Hydrobiology, Chinese Academy of Sciences, Wuhan 430072, China. Tel.: +86 27 68780792; fax: +86 27 68780123.
E-mail address: zhangqy@ihb.ac.cn (Q.-Y. Zhang).

http://dx.doi.org/10.1016/j.dci.2014.05.019
0145-305X/

the thymus. Expressed sequence tags (ESTs) strategy based on cDNA library was employed, because it has provided a powerful platform for gene discovery, especially in organisms that have little genomic information (Giallourakis et al., 2013). Although conventional Sanger sequencing is time consuming, it yields high-quality and long reads, which is reliable for the assembly of gene isoforms (Au et al., 2013), and is therefore still used as an effective strategy in the next-generation sequencing era.

In the present study, we constructed a cDNA library from the ADRV-induced thymus. Through EST survey, we investigated the characteristics of molecules associated with innate and adaptive immunity, with a focus on three representatives: immunoglobulin heavy chains (IgM, IgY, and IgD), IFN-inducible protein 6 (IFI6), and T-cell receptor beta chain (TCRβ). Detailed research concerned on the structural features, expression profiles, splicing patterns, as well as their potential evolutionary implications. This study represents an important starting point for characterizing the function and evolution of immune system in this poorly understood species, as well as bolsters comparative studies in amphibian taxa.

2. Materials and methods

2.1. Salamanders, cells, and virus

Chinese giant salamanders weighing about 120 g were obtained from a farm in Jiangxi, China. The salamanders were reared in an aerated freshwater tank at 22 °C for 2 weeks prior to experiment. Thymocytes from the salamanders were cultured at 20 °C in medium 199 with 10% FBS. *Andrias davidianus* ranavirus (ADRV) was propagated in *Epithelioma papulosum* cyprini (EPC) cells as described previously (Chen et al., 2013).

2.2. cDNA library construction

Chinese giant salamanders were intraperitoneally injected with 1 ml serum-free medium 199 containing ADRV ($10^{6.5}$ $TCID_{50}$/ml). On 12 days after injection, the salamanders displayed hemorrhage and swelling of the skin (Chen et al., 2013). To construct a cDNA library, the thymus was sampled from the challenged individual. Total RNA was extracted with Trizol reagent (Invitrogen) and mRNA was isolated with Oligotex-dT30 mRNA kits (Takara). The cDNA library was constructed with In-Fusion SMARTer cDNA library construction kit (Clontech) following the manufacturer's instruction. Briefly, double stranded cDNA was synthesized from mRNA, size-fractionated through the CHROMA SPIN+TE-1000 column, ligated into pSMART2IFD linearized vector, and transformed into *Escherichia coli* cells. Randomly selected clones were subjected to PCR amplification to identify positive recombinants and then single-pass sequenced on ABI 3730 DNA sequencer (Applied Biosystems).

2.3. EST assembly and annotations

After trimming vector and adapter sequences using VecScreen program, the ESTs (>100 bp) were assembled using Phrap program. To assess sequence similarity with known genes, the assembled sequences were searched against the NCBI non-redundant protein and nucleotide databases using BLASTX and BLASTN with a cutoff *E*-value of $1\ e^{-5}$. Additionally, these sequences were compared with the EST databases of Chinese giant salamander, axolotl, and *Xenopus*, respectively. *E*-value from the first identified hit was used to assign a putative identity to the genes. Next, the genes that had matches in non-redundant databases were assigned to GO terms using Blast2GO software (Conesa et al., 2005), and the results were submitted to the WEGO program to perform GO functional classification (Ye et al., 2006). Pathways annotation was carried out using the KEGG (Kyoto Encyclopedia of Genes and Genomes) database (Moriya et al., 2007).

2.4. Sequence analyses of selected genes

The deduced amino acid sequences of the immune genes were analyzed for the presence of a signal peptide with SignaP 3.0 software, and of *N*-linked glycosylation sites with the NetNGlyc 1.0 server. The variable (V) and constant (C) domains of TCRβ and IgH genes were analyzed using the IMGT (the international ImMunoGeneTics information system) standardisation numbering (Li et al., 2013). The Ig V_H families were classified based on the criterion that members of each family share 75% or more identity (Giudicelli and Lefranc, 1999). Multiple sequence alignments were generated using Clustal X. Phylogenetic analysis was performed using the Neighbor-Joining method with MEGA 5 (Tamura et al., 2007). The phylogenetic tree of IgH constant region sequences was constructed using the entire constant region, except that the first four constant domains were used for IgD genes of lower vertebrates. The three-dimensional structure of IgD was predicted by homology modeling using Swiss-Model server and the figures were visualized by DeepView software (Kiefer et al., 2009). The crystal structure of human IgD was used as template model (PDB entries: 1IGY).

2.5. Expression profile analyses of selected genes

To examine the tissue distribution of selected gene products, three healthy salamanders were sampled to isolate eight tissues including liver, spleen, kidney, thymus, intestine, skin, muscle and testis. Total RNA was exacted from each tissue separately and used for RT-PCR analysis. The PCR conditions were as follows: 95 °C for 5 min, 95 °C for 30 s, 52 °C for 30 s, and 72 °C for 30 s for 30 cycles, followed by 72 °C for 10 min. All primers were list in Supplemental Table 1.

To determine the relative expression of selected gene products following *in vivo* or *in vitro* stimulation, three salamanders were challenged with ADRV ($1 \times 10^{6.5}$ $TCID_{50}$/ml) as described previously (Zhu et al., 2014). The control was stimulated with sterilized saline (0.9% Sodium Chloride). Five tissues (liver, spleen, kidney, intestine, and thymus) were sampled and total RNA was exacted from each tissue separately. Real-time PCR assays of gene expression were performed as described previously (Zhu et al., 2013). The relative expression levels of target genes were determined using β-actin as an internal control with the comparative Ct ($2^{-\Delta\Delta Ct}$) method and expressed as the mean ± SD of the results obtained from three individuals. For *in vitro* stimulation experiment, Chinese giant salamander thymus cells (CGST) cultured in 25 cm^2 culture plates were incubated with ADRV at a multiplicity of infection (MOI) of 0.05, or with 250 μg/ml LPS (Sigma). The cells treated with FBS-free 199 were used as control in parallel. At various times (6, 12, 24, 48 and 72 h) post-infection, the cellular RNA was extracted and used for real-time PCR as described above.

2.6. Western blotting for IgY isoforms detection

The peptide CGIKTFPAVLQKSPT derived from the C_H1 domain of IgY was synthesized and used to immunize rabbits. A polyclonal IgY antibody was obtained and purified (GenScript, Nanjing). Serum samples from Chinese giant salamanders were separated by 12% SDS–PAGE and transferred to polyvinyl difluoride membranes (Millipore). Membranes were incubated with anti-IgY antibody at 1:1000 in TBST buffer containing 1% milk (25 mM Tris–HCl pH 7.5, 150 mM NaCl, 0.1% Tween 20), with final detection provided by alkaline phosphatase-conjugated goat anti-rabbit antibody (Vector).

2.7. Subcellular localization and antiviral activity evaluation of IFI6 gene

To determine the subcellular localization of IFI6 and its splice variant, EPC cells were grown on microscopic coverslips in 6-well plates, and cotransfected with 2 μg pEGFP-IFI6 or pEGFP-IFI6-sv, together with 2 μg pDsRed2-Mito. After 48 h, the cells were washed with PBS, fixed in 4% paraformaldehyde for 30 min, and stained with Hoechst 33342 (Sigma) for 5 min. The cells were then visualized under a Leica DM IRB fluorescence microscope (objective 100×).

To address whether the full-length and truncated IFI6 forms were functional, overexpression assay were performed. CGST cells seeded in 6-well plates were transfected with 4 μg pcDNA3.1-IFI6, pcDNA3.1-IFI6-sv or empty vector (pcDNA3.1) control. After 24 h, the cells were infected with ADRV (0.1 MOI), or with SMRV (0.3 MOI), and incubated for 24 h. The cell monolayers were subjected to total RNA extraction for real-time PCR assay of viral replication. The supernatant aliquots were subjected to 50% tissue culture infective dose ($TCID_{50}$) assay of viral titers as described previously (Chen et al., 2013).

2.8. CDR3 spectratyping analyses of TCRβ gene

Two-round PCR amplifications were performed to analyze CDR3 length spectratyping of TCRβ genes (Boudinot et al., 2002). Briefly, the first-round PCR was conducted using a forward primer specific for each Vβ family, together with a reverse primer specific for Cβ sequence (Supplemental Table 1), which amplified sequences with a given Vβ, but with different CDR3 sizes. Then these PCR products were used as template in the second-round PCR with fluorescent Cβ-specific primers. The runoff products were size-separated on ABI 3730 sequencer and CDR3 length distributions were detected using GeneMapper software.

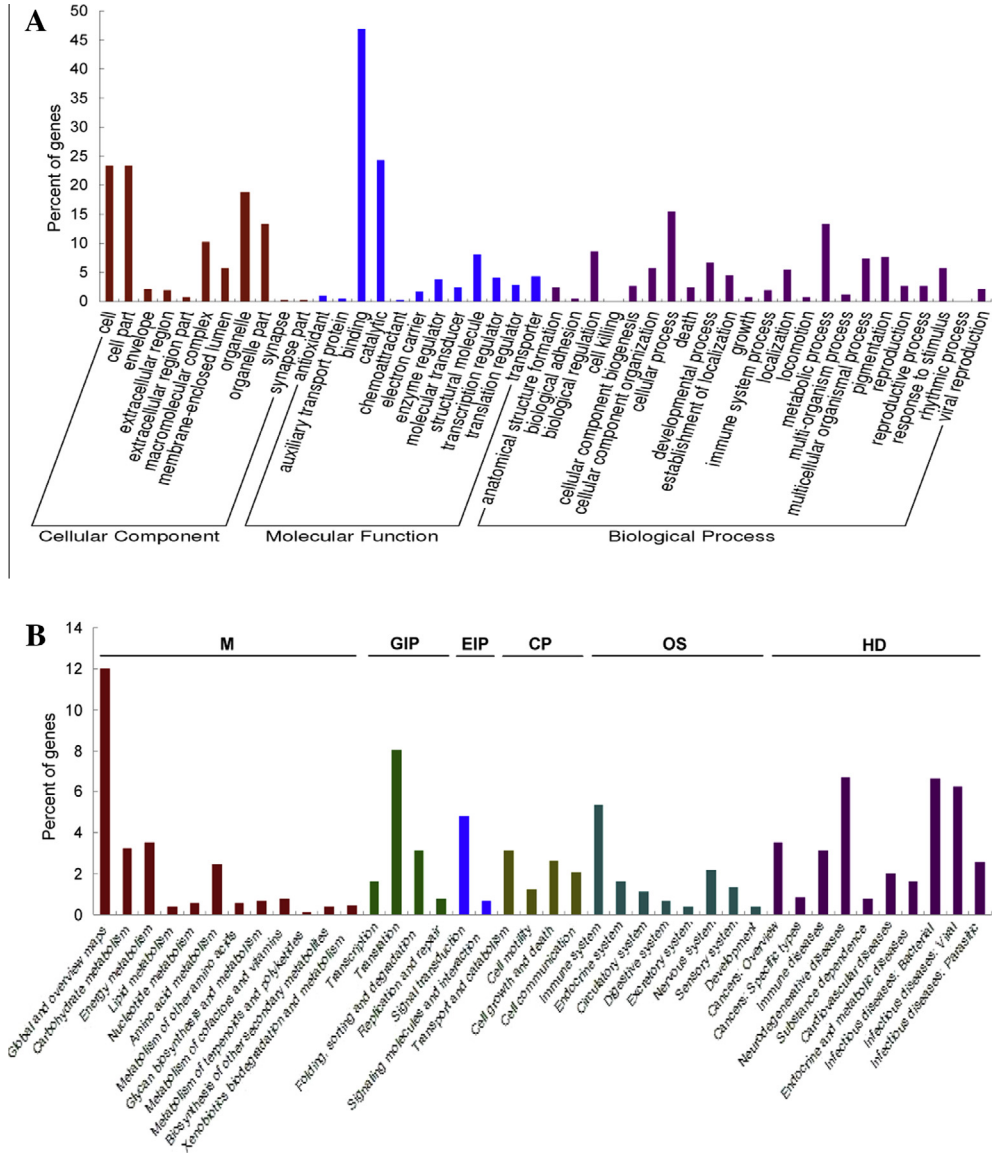

Fig. 1. Functional classification of assembled sequences. (A) GO annotation of the sequences according to three categories: biological process, molecular function, and cellular component. The *x*-axis represents GO terms at level 2 and *y*-axis represents the percentage of sequences assigned to each term. (B) KEGG pathway assignments of the sequences in six categories including metabolism (M), genetic information processing (GIP), environmental information processing (EIP), cellular processes (CP), organismal systems (OS), and human diseases (HD). The *x*-axis represents enriched KEGG pathways and *y*-axis represents the percentage of sequences in each pathway.

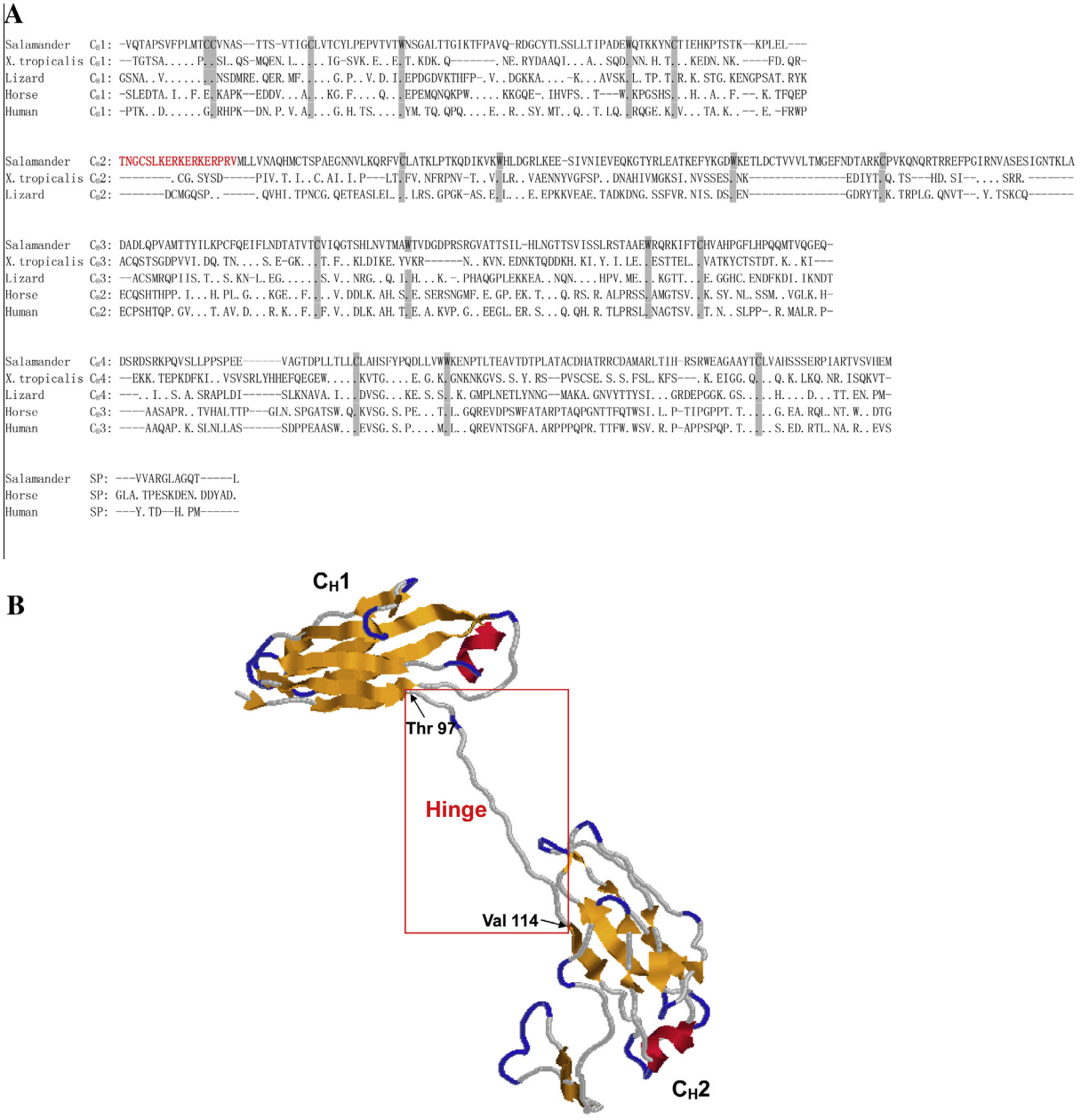

Fig. 2. Sequence and model for IgD constant region. (A) Alignment of *A. davidianus* IgD with those of other species. IgD constant region is composed of four domains (C_H1–4) and a secretory tail (SP), in contrast to the eight-domain structure in other amphibian IgD (only first four domains shown). A putative 18-aa hinge region (bold) is located between the C_H1 and C_H2 domains. The Cys and Try (shaded) are conserved in each domain. Bars and dots indicate identical amino acids and gaps, respectively. (B) Predicated structural model of IgD C_H1–2. Ribbon cartoon diagram displays a putative hinge (box) linking the two domains, which involves residues Thr97 to Val114 (arrow). α-Helices are shown as helical ribbons (red), and β-strands are represented as thick arrows (yellow). (For interpretation of the references to color in this figure legend, the reader is referred to the web version of this article.)

3. Results

3.1. The thymus cDNA library is enriched for immune-related genes

The thymus cDNA library was subjected to EST survey, similarity searches, and functional annotation to explore host genes potentially involved in immune response.

Library screening yielded 1197 high-quality ESTs (Genbank accession numbers: JZ574185–JZ575381), representing 812 unique sequences. Of these, 730 genes were novel for Chinese giant salamander, a substantial expansion of existing genetic resource. Sequence comparisons revealed that 280 and 213 genes had homologs in the axolotl and *Xenopus*, respectively; 120 genes were common among the three species, while 160 appeared to be urodela-specific sequences. Functional annotations showed that 556 genes were classified into GO terms (Fig. 1A), and 456 were mapped into KEGG pathways (Fig. 1B). Accordingly, 137 genes were assigned to immune-related processes (Supplemental Table 2), including the main components of adaptive immunity (e.g., MHC, Igs, CD3, and proteasomes) and innate immunity (e.g., C3, IL-8, lysozyme, cathepsin, and IFN-related genes), as well as apoptosis-related molecules (e.g., caspase 3, CARD9, and ANXV). The discovery of a

complex set of immune genes in this library implied that there is a robust immune system in this primitive amphibian.

Among the identified genes, three have attracted particular attention: IgH, the key components of adaptive immunity; IFI6, one of the first identified IFN-stimulated genes (ISGs); TCRβ, the most abundant genes found in this library. The characteristics of these selected genes will be described in more detail below.

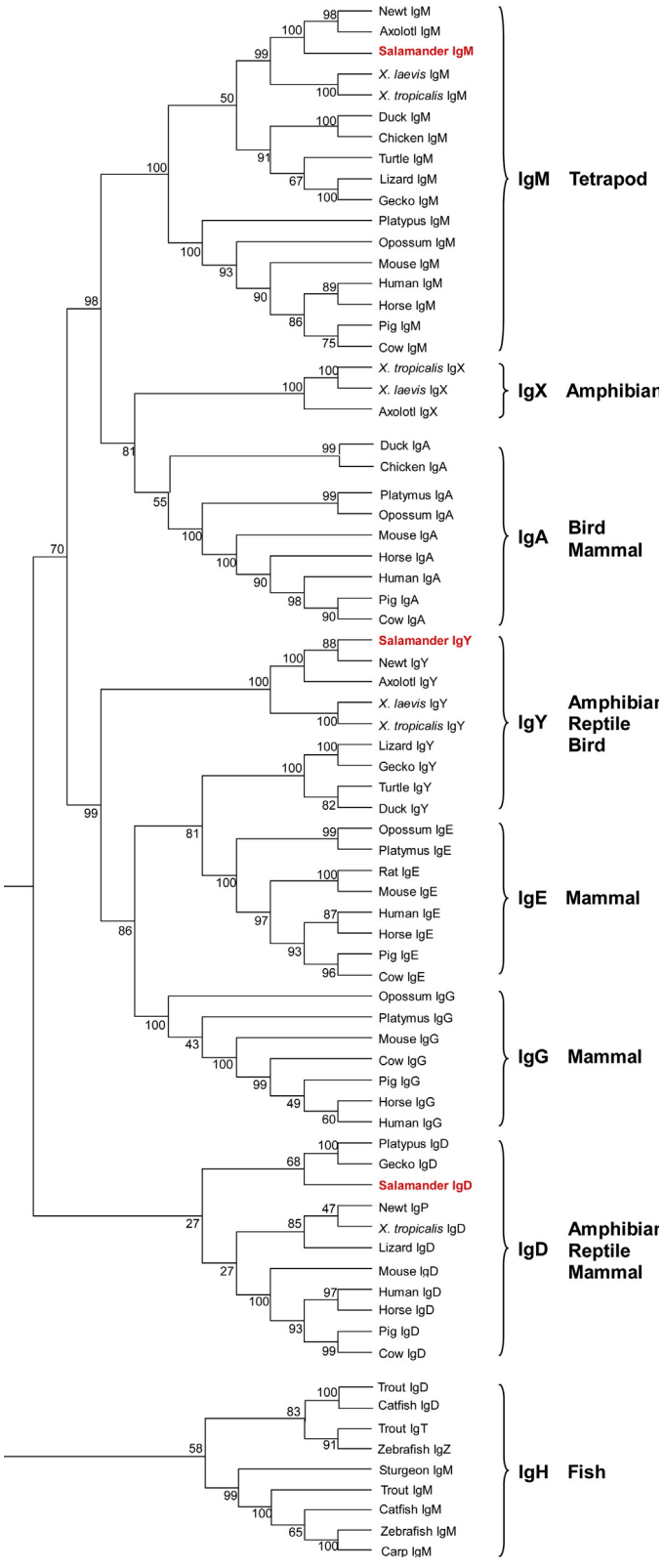

3.2. *A. davidianus* IgD is distinct from other amphibian IgD, while IgM and IgY are in common with amphibian homologs

Three IgH isotypes, namely IgD, IgM, and IgY, were identified and their structural features, expression profiles, and splicing patterns were investigated.

3.2.1. Sequence analyses of IgD, IgM, and IgY

The deduced constant regions of three IgH isotypes were aligned with the respective vertebrate sequences. Notwithstanding IgD (Genbank accession number: KJ686312) shows a conserved distribution of Cys residue contributing to intra- and inter-chain disulfide bonds, it exhibits a structural pattern distinct from that of known amphibian IgD with two respects: (1) it contains only four putative C_H domains (C_H1–C_H4), which is significantly shorter in length than its orthologs from cold-blooded vertebrates (Fig. 2A); (2) it is essential to note that an 18-aa interconnecting loop (amino acid 97–114) lies between C_H1 and C_H2 (Fig. 2B), which may potentially serve as a hinge region. This region is structurally similar to mammalian equivalents, comprising one Cys residue, several charged residues (e.g., Lys, Glu, Ser, and Thr), and a repetitive sequence (KER). In contrast, IgM (Genbank accession numbers: KJ686309–KJ686310) constant region shows a high degree of conservation both in terms of the number of C_H domains (four) and the content of functionally important residues across species over long phylogenetic distances (Supplemental Fig. 1A). The secretory tail preserves a canonical *N*-linked glycosylation site implying the capacity of secreted IgM to form polymers, and the transmembrane tail contains essential polar residues (e.g., Thr, Ser, and Tyr) required for Igα/Igβ coreceptor association. Similar observation was made for IgY (Genbank accession numbers: KJ686315–KJ686318), which harbors four full-length transcripts resulted from the expression of different alleles (Supplemental Fig. 1B). Phylogenetic analysis showed that vertebrates IgH chains are grouped into eight distinct clusters according to the isotypes, with the exception of fish sequences. *A. davidianus* IgM and IgY cluster most closely with their respective homologs from other amphibians, whereas IgD of this species appears to be closer related to those of the platypus and lizard than to amphibians (Fig. 3A).

Next, the variable regions of IgH were aligned, revealing the presence of seven distinct V_H families (V_H1-V_H7) (Genbank accession numbers: KJ686324–KJ686330) (Supplemental Fig. 1C). All V_H families contain conserved residues for Ig fold and consensus

Fig. 3. Phylogenetic relationships of IgH constant genes from representative vertebrates. All sequences are separated according to Ig classes: IgM, IgX, IgA, IgY, IgE, IgG and IgD, except the fish sequences. Note that *A. davidianus* IgM and IgY (bold) are tightly clustered with their respective amphibian homologs, whereas IgD (bold) is more closely related to those of the platypus and lizard than to amphibians. GenBank accession numbers of sequences are as follows: IgM: *X. laevis*, J03631; *X. tropicalis*, AAH89670; Axolotl, A46532; Newt, CAE02685; Duck, AJ314754; Chicken, X01613; Turtle, ACU45376; Lizard, ABV66128; Gecko, ABY74509; Platypus, AY168639; Mouse, J00443; Opossum, AAD24482; Human, AAV39625; Horse, AAU09792; Pig, BAI82566; Cow, AAN60017; Sturgeon, AHB18162; Trout, AAW66973; Catfish, X52617; IgY: *X. laevis*, X15114; *X. tropicalis*, AAH89679; Axolotl, CAA49247; Newt, CAE02686; Lizard, ABV66132; Gecko, ACF60236; Turtle, ACU45374; Duck, X78273; IgD: *X. tropicalis*, DQ350886; Newt, AM295004; Lizard, ABV66130; Gecko, ABY67439; Platypus, ACD31540; Mouse, J00449; Human, K02879; Horse, AY631942; Pig, AAN03672; Cow, AAN03673; Trout, AAW66977; Catfish, U67437; IgX: *X. laevis*, BC072981; *X. tropicalis*, AAI57651; Axolotl, CAO82107; IgA: Duck, U27222; Chicken, A46507; Platypus, AY055778; Opossum, AAD21190; Mouse, J00475; Horse, AAP80145; Human, J00220; Pig, ADD51207; Cow, AF109167; IgE: Platymus, AY055780; Opossum, AAC79674; Rat, AAA41365; Mouse, X01857; Horse, AAA85662; Human, J00222; Pig, AAC48776; Cow, AY221098; IgG: Platypus, AY055781; Opossum, AAC79675; Mouse, J00453; Human, J00228; Horse, CAC44760; Pig, AAA51294; Cow, ABE68619; IgT: Trout, AAW66981; IgZ: Zebrafish, AY643750.

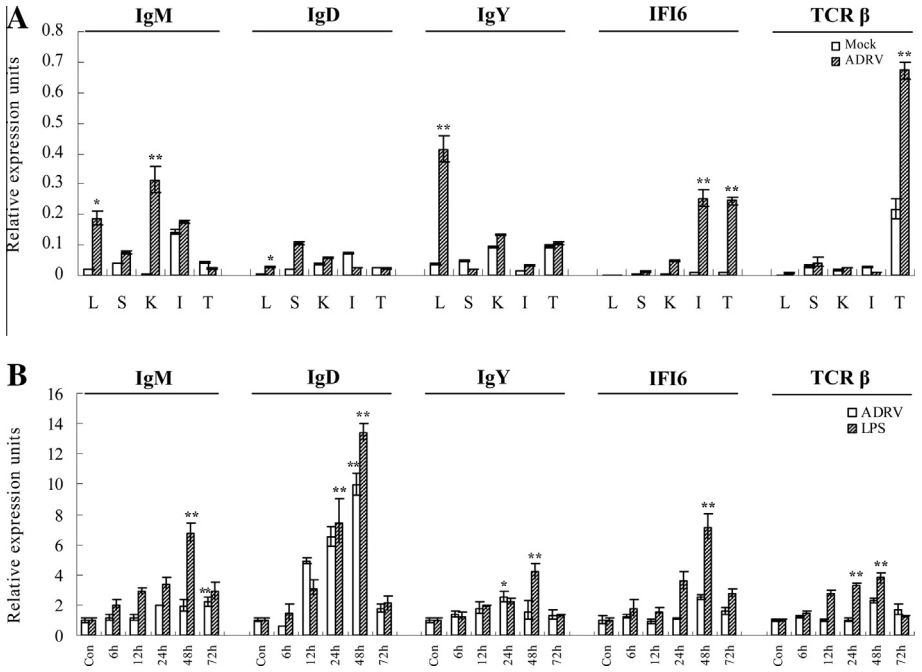

Fig. 4. Expression profiles of selected immune genes after *in vivo* and *in vitro* stimulation. (A) Real-time PCR analysis of the expression levels of IgM, IgD, IgY, IFI6, and TCRβ in mock-infected and ADRV-infected tissues [liver (L), spleen (S), kidney (K), intestine (I), thymus (T)]. Values were expressed as a ratio relative to β-actin levels in the same samples. (B) Real-time PCR analysis of gene expression in CGST cells treated with ADRV or LPS for the indicated times. Values were normalized against that of the control cells (Con), and expressed as mean ± SD ($n = 3$). Statistical analysis was performed using Student' *t*-test. *, $P < 0.05$; **, $P < 0.005$.

motifs (WIRQ, YYC, and WGXGT), however, they display great divergent in CDR3 length (mean: 11.5 aa). Phylogenetic analysis indicated that the seven V_H families fall into three mammalian V_H clans (clan I–III) (data not shown), suggesting that Chinese giant salamander utilizes a large number of germline V_H families to generate a diversified heavy chain repertoire.

3.2.2. Expression profiles of IgD, IgM, and IgY

Expression patterns of the three isotypes were assessed *in vitro* and *in vivo*. Overall the transcript levels of all isotypes showed significant up-regulation after ADRV stimulation, with the most obvious change of IgM, IgD, and IgY found in the kidney (122.8-fold), spleen (5.3-fold), and liver (11.1-fold), respectively (Fig. 4A). Likewise, their expression levels were evaluated in ADRV-challenged cells. IgM mRNA increased gradually from 6 to 72 h post-infection, while IgD and IgY mRNA increased respectively to the peak at 48 h and 24 h, then recovered to the normal level at 72 h. Similar inductions were observed in LPS-treated cells (Fig. 4B), clarifying their immunological importance.

3.2.3. Splicing patterns of IgD, IgM, and IgY

In addition to the full-length forms mentioned above, three IgH isotypes also occurred in multiple truncated forms with sequence characteristics indicative of alternative splicing. IgY comprises five splice variants (termed IgY-sv1-5; Genbank accession numbers: KJ686319–KJ686323), each arising from the exclusion of one or two C_H domains. An important point to note is that IgY-sv5 is devoid of the Fc region (C_H3 and C_H4), thus resembling IgY(ΔFc) (Fig. 5A). Such a short IgY form was somewhat unexpected since it appears restricted to several birds and reptiles. To confirm the existence of IgY isoforms, their mRNA expressions in tissues were measured by RT-PCR (Fig. 5A, left panel). Results revealed that both intact and truncated transcripts showed a similar, broad tissue distribution, and enriched in the lymphoid tissues. Furthermore, their presence at the protein level was determined by Western blot with polyclonal antibody specific for C_H1 (Fig. 5A, right panel). This analysis rendered two dominant bands of ~60 kDa, representing full-length IgY. Also, as expected, IgY-sv5 (~33 kDa) was detected, although in a weaker fashion than the full-length forms. Three additional weak bands were observed, representing IgY-sv1 (~47 kDa), IgY-sv2 (~45 kDa), and IgY-sv3 (~36 kDa), respectively, whereas IgY-sv4 was not detectable because of its lack of C_H1. Like IgY, IgM and IgD also underwent alternatively splicing that led to one and two truncated variants (Genbank accession numbers: KJ686311, KJ686313, KJ686314), respectively (Fig. 5B); moreover, the long and short forms co-expressed in various tissues. Thus, these data indicate that Chinese giant salamander is most likely to utilize alternative splicing machinery to produce IgH diversification.

3.3. IFI6 occurs in two forms differing in functional features

IFI6, an ISG that may protect virus-infected cells from apoptosis (Parker and Porter, 2004), existed as two forms in this library. Thus, their divergences in subcellular localization and antiviral effect were examined.

3.3.1. Sequence analyses of IFI6

IFI6 (Genbank accession number: KJ686342) encodes a putative hydrophobic protein of low molecular weight (130 aa), consisting of five components: a leader peptide (LP), two transmembrane domains (TM1, TM2), and two hydrophilic domains (HL1, HL2). The transmembrane domains are the most highly conserved between species, reflecting their likely functional importance. The predicted protein sequence shares 42–62% similarity with its mammalian counterparts. The transcriptional pattern assessment revealed that IFI6 expression in the thymus and intestine were elevated upon stimulation with ADRV (Fig. 4A). Also, its expression in CGST cells increased after treatment with either ADRV or LPS, indicating that IFI6 could be induced by pathogens challenge (Fig. 4B). Additionally, a short form termed IFI6-sv (Genbank accession number: KJ686343) was also found, which maintains the same reading

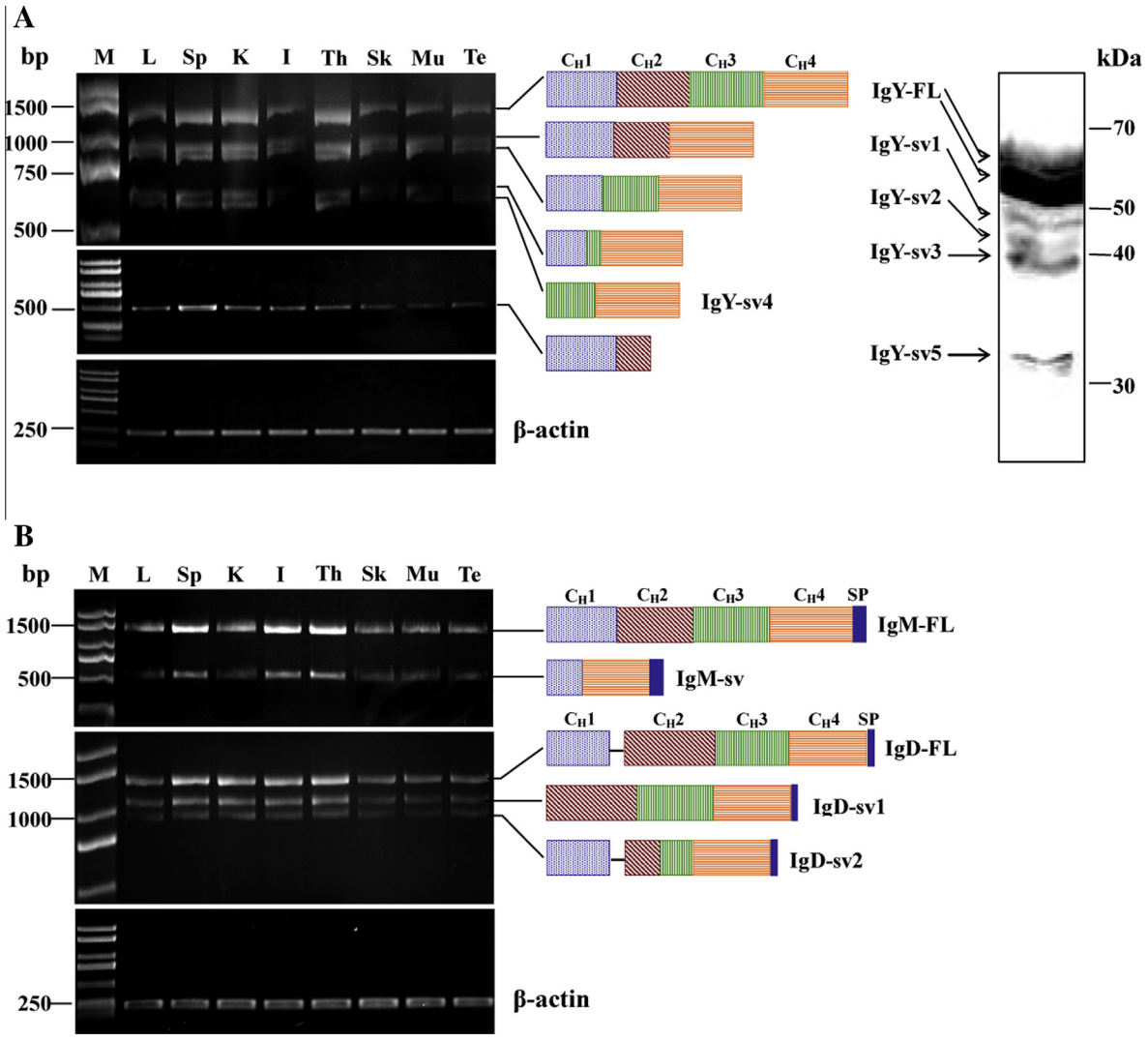

Fig. 5. Expression and splicing patterns of three IgH isotypes. (A) RT-PCR amplification of IgY constant region in tissues [liver (L), spleen (Sp), kidney (K), intestine (I), thymus (Th), skin (Sk), muscle (Mu), testis (Te)]. Five bands were observed: the biggest one represents full-length form (IgY-FL), and the others represent splice variants (IgY-sv1 to IgY-sv5), as shown in the diagrams. The C_H1-specific antibody detected IgY forms except IgY-sv4 in Western blot analysis. M: 2-kb ladder. β-Actin: control. (B) RT-PCR detected two IgM and three IgD bands in tissues: the bigger ones represent full-length forms (IgM-FL and IgD-FL), and the smaller ones represent splice variants (IgM-sv, IgD-sv1, and IgD-sv2). SP: secretory tailpiece. Dash: hinge region.

frame as the full-length sequence, despite the fact that the LP, HL1, and part of the TM1 domain were spliced out. RT-PCR detection confirmed the existence of the two IFI6 forms in a variety of tissues (Fig. 6A).

3.3.2. Subcellular localization of IFI6

Using a GFP reporter system, it was demonstrated that the intact and truncated IFI6 adopted different subcellular distributions: the full-length form was present in mitochondria as seen in mammals, whereas IFI6-sv was diffusely distributed throughout the cytoplasm with absence from mitochondria (Fig. 6B), suggesting that the N-terminal region represents a putative targeting peptide that is indispensable for its localization.

3.3.3. Antiviral effect of IFI6

Upon transfection into CGST cells, it was proved that the divergence between the two forms was also reflected by their ability to restrict virus replication. As illustrated in Fig 6C, ectopically expressed IFI6 led to reduction in the expression of ADRV major capsid protein (MCP) (2.5-fold against empty vector) and SMRV nucleoprotein (N) (3.3-fold against empty vector). Consistently, the titers of ADRV and SMRV in IFI6-transfected cells decreased about 13-fold ($10^{6.5}$ $TCID_{50}$/ml versus $10^{5.4}$ $TCID_{50}$/ml) and 251-fold ($10^{7.9}$ $TCID_{50}$/ml versus $10^{5.5}$ $TCID_{50}$/ml), respectively (Fig. 6D). In comparison, IFI6-sv overexpression yielded a moderate decrease in the virus production (Fig. 6C and D). It therefore appears that IFI6 exerts antiviral effect by targeting to mitochondria, implicating a similar effect both in amphibians and mammals during virus infection.

3.4. TCRβ displays diverse repertoire

During the library screening, TCRβ gene stands out with the most frequent ESTs found in the thymus.

3.4.1. Sequence analyses of TCRβ

At least 11 full-length TCRβ transcripts (designated TCRβ1-11; Genbank accession numbers: KJ686331–KJ686341) were isolated, all of which have canonical structure: the conserved Cys residues involved in intrachain disulfide bond, the conserved motif of YYCA

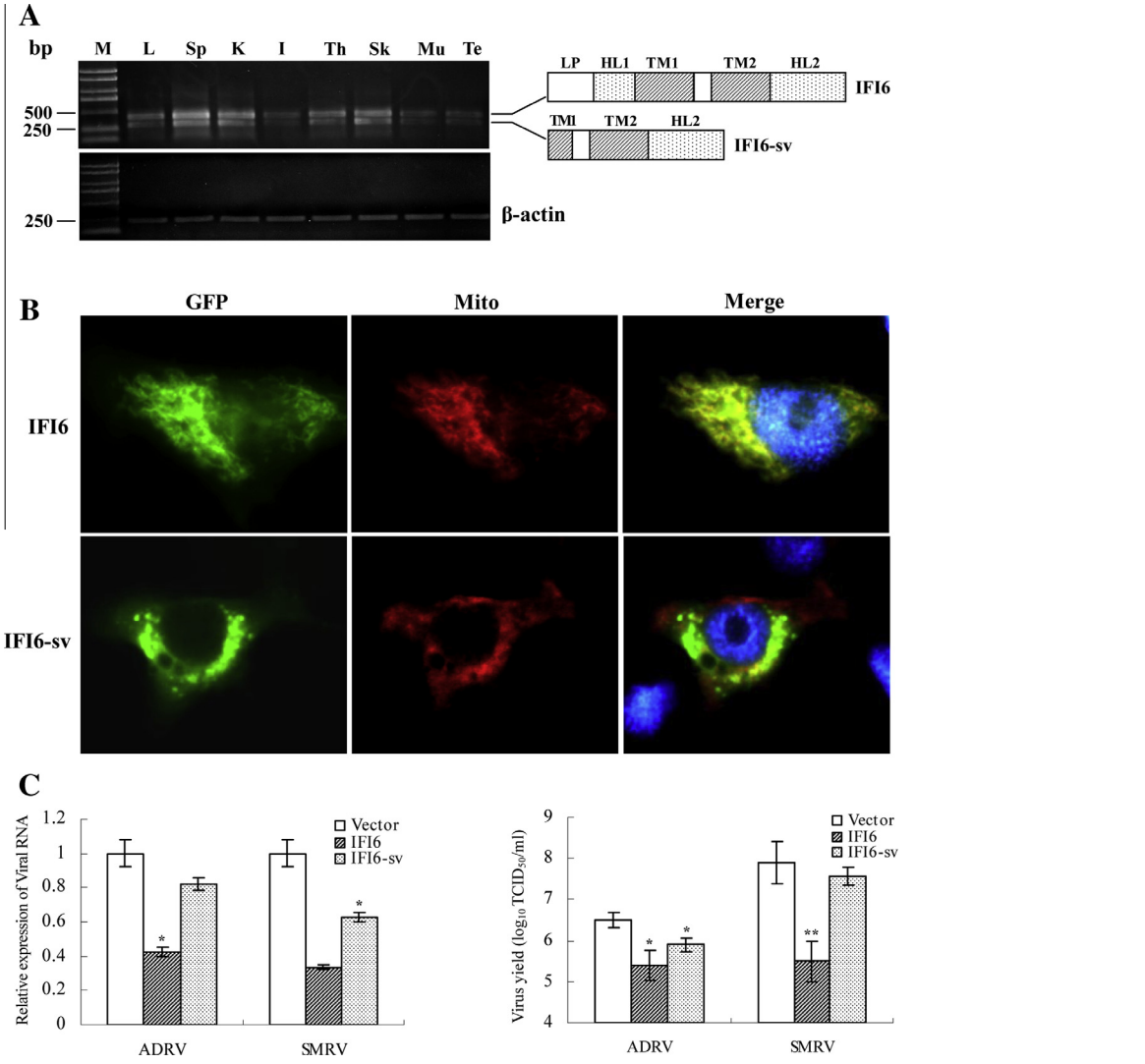

Fig. 6. Tissue distribution, subcellular localization, and antiviral activity of IFI6 isoforms. (A) RT-PCR amplification in tissues [liver (L), spleen (Sp), kidney (K), intestine (I), thymus (Th), skin (Sk), muscle (Mu), testis (Te)] detected two bands, corresponding to the intact and truncated IFI6 (IFI6-sv). IFI6 contains five domains: a leader peptide (LP), two hydrophilic domains (HL1, HL2), and two transmembrane domains (TM1, TM2). M: 2-kb ladder. β-Actin: control. (B) IFI6 (EGFP, green) colocalized (Merge, yellow) with mitochondria (Mito, Red), whereas IFI6-sv (EGFP, green) excluded from mitochondria (Mito, Red). Blue fluorescence showed the nuclei stained by Hoechst 33342. (C) Real-time PCR analysis of the expression of ADRV MCP and SMRV N in CGST cells transfected with IFI6, IFI6-sv or empty vector control, which were shown as fold increase values relative to the control (set as 1). (D) $TCID_{50}$ measurement of virus yields in the cells described in (C). The results are representative of three independent experiments performed in triplicate (means ± SD). *, $P < 0.05$; **, $P < 0.005$.

in the FR3, and the FGXG motif in the FR4 (Supplemental Fig. 2). Sequences comparison clearly defines four distinct Vβ and three Cβ segments, suggesting the potential V/C combinatorial diversity. To get insight into TCRβ diversity, the CDR3 length spectratyping was performed, since the CDR3 loop is the most critical TCR sequence for determining antigenic combining site diversity. It was found that the histograms of all Vβ segments (Vβ1-4) show a Gaussian distribution in naive individuals (Fig. 7), as typically observed for vertebrate TCRβ. Thus, the above results indicate that Chinese giant salamander harbors a diverse and polyclonal TCRβ repertoire.

3.4.2. Expression profiles of TCRβ

The expression pattern of TCRβ in various tissues was assessed. The highest level of TCRβ mRNA was detected in the thymus, reflecting the primary lymphoid nature of this organ. Moreover, upregulation of TCRβ expression was observed in the immune tissues after ADRV infection (Fig. 4A). In CGST cells, its expression level increased within 48 h after stimulation with ADRV or LPS, indicating the roles of TCRβ in the immune defense against pathogens (Fig. 4B).

4. Discussion

A cDNA library survey was conducted with the thymus from Chinese giant salamander upon ranavirus stimulation. The more detailed study of representative immune genes (IgM, IgD, IgY, IFI6, and TCRβ) reveals some differences compared to their respective counterparts from other vertebrates. This study provides a global perspective on immune characteristics of this amphibian, which represents a relevant contribution to the knowledge of immune systems of lower vertebrates.

Mining the library enabled the identification of 812 unique sequences, of which 730 were novel for Chinese giant salamander. Prior to this study, only a small number of ESTs (307 ESTs) in NCBI were available for this species, thus our data enrich the existing

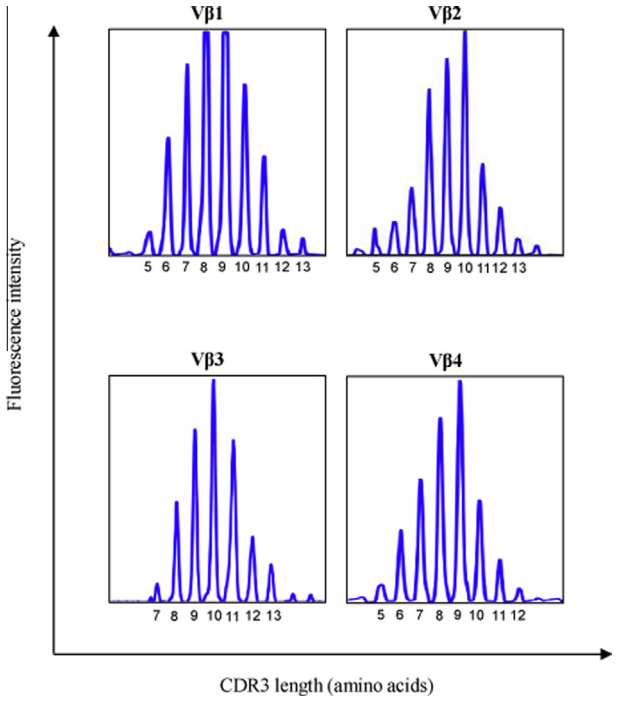

Fig. 7. Immunoscope analysis of TCRβ in naive spleen. All four Vβ families (Vβ1-4) display a type Gaussian profile. Each profile represents the CDR3 length distribution for a given Vβ family. The *x*-axis shows CDR3 size and *y*-axis shows relative fluorescence intensity of the peaks.

genetic resources. A total of 137 candidate genes were potentially involved in immune responses, a high ratio most likely due to an effective stimulation with ranavirus, since ranavirus infection can induce robust immune response in amphibians (Grayfer et al., 2014; Ryazantsev et al., 2013). It has long been recognized that amphibian thymus is the primary lymphoid organ (Chen and Robert, 2011). Until now, however, studies have concentrated on the organization and development of the thymus (Lee et al., 2013). Here, we developed thymus library as a tool to identify host genes relevant to ranavirus resistance. As a result, an important set of innate and adaptive immune components were generated, which are suggestive of the significant roles that the thymus plays in immune defense. The wealth of sequence information provides a valuable resource for future studies on this species.

One interesting finding in this study is that IgD of this species displays a structural pattern strikingly different from that previously described for amphibian species. First, IgD contains a putative hinge linking the C_H1 and C_H2 domains. To our knowledge, it represents the first hinge-containing IgD in nonmammalian tetrapods, since no hinges have been reported in the lower vertebrate IgD sequenced to date. The hinge region is critical for Ig function: it confers conformational flexibility, thus facilitating antigen binding and triggering effector functions (Ryazantsev et al., 2013). This segment is generally present in mammalian Igs, but it is assumed to be evolved in lower vertebrates. Our finding supports this notion, in accordance with the previous study of *Xenopus* IgF (Zhao et al., 2006). The hinge region of *A. davidianus* IgD shares structural properties in common with that of mammalian IgD, such as repetitive sequence. The presence of distinct repeat is generally seen in Ig hinges (e.g., NTKP in *Xenopus* and VKPT in fugu) (Savan et al., 2005; Zhao et al., 2006), which appears to contribute to evolutionary instability and genetic diversification of this region. Second, *A. davidianus* IgD possesses a much shorter constant region than other amphibian IgD. IgD in various vertebrates displays remarkable structural plasticity in terms of the number of C_H domains (Danilova et al., 2005; Edholm et al., 2011; Ohta and Flajnik, 2006). It tends to have more C_H domains in non-mammalian vertebrates (eight or more C_H) than in placental mammals (two or three C_H) (Li et al., 2012; Ramirez-Gomez et al., 2012; Zhao et al., 2009). *A. davidianus* IgD has only four C_H domains, which is more similar to mammalian counterparts in size. Overall, our study describes an unusual IgD isotype which has not been reported in amphibian species.

Another striking finding is that IgY(ΔFc) is present in this species. Such a truncated IgY form has been suggested to neutralize pathogens without initiation of inflammatory responses (Humphrey et al., 2004), due to its lack of the last two C_H domains corresponding to the Fc region. It has been only found in several birds and reptiles, such as duck, lizard, and snake (Magor et al., 1994; Wang et al., 2012; Wei et al., 2009), and no IgY(ΔFc) sequence has so far been obtained in amphibians, although the presence of IgY(ΔFc)-like antibody has been reported in the bullfrog (*Rana catesbeiana*) (Marchalonis and Edelman, 1966). The mechanism for the formation of *A. davidianus* IgY(ΔFc) is similar to the case of lizard (Wei et al., 2009), in which the truncation is a result of alternative splicing. But it is different from that described for the duck IgY(ΔFc), which is generated by the usage of a small additional exon that occurs in the C_H2–C_H3 intron. In IgY(ΔFc) transcript, an alternative 5′ splice site located within C_H2 exon is chosen, leading to the exclusion of a part of C_H2 domain. A 16-aa tail (LCVGISSVQSYYHSAI) and 3′-untranslated region are immediately adjacent to C_H2. It thus seems that IgY(ΔFc) is spliced based on the recognition of the cleavage/polyadenylation site downstream of the donor site. Furthermore, this study shows evidence for the presence of IgY(ΔFc) at both the mRNA and protein level, but its functional significance during viral infection remains to be addressed. As observed for IgY, IgM and IgD also underwent alternatively splicing. The coexistence of multiple isoforms in Chinese giant salamander suggests that alternative splicing as a mechanism for Ig heterogeneity reported in mammals is also employed in amphibians. It is speculated that different IgH isotypes, together with their multiple forms, fulfill particular needs for the adaptive immune system. Since amphibians are exposed to a broad range of pathogens in harsh living conditions, the diversification of IgH may enable hosts to combat various pathogens with great precision.

Additionally, this study is the first to describe IFI6 gene in amphibian species. IFI6 is a small ISG belonging to the FAM14 family with largely unknown function (Cheriyath et al., 2011). It has been shown to antagonize mitochondria-mediated apoptosis during viral infection (Parker and Porter, 2004). While extensive studies on mammalian IFI6 are well reported, little is known about the function or role of its counterparts in lower vertebrates. Two IFI6 isoforms, intact and truncated, were co-expressed in Chinese giant salamander. IFI6 full length is localized to mitochondria, following the same pattern as in mammals, but this localization does not apply for the N-terminally truncated form. Moreover, the splice variant shows impaired antiviral effect, indicating that it might be defective in biological activity. These observations provide additional understanding of function exerted by the IFI6 family in lower vertebrates. Moreover, TCRβ has all the hallmarks of typical TCRβ sequences: various V/C combinations and Gaussian distributions of CDR3 length, which imply that this species possesses a polyclonal and diverse T cell repertoire. Further studies will be necessary to determine the functionality of T cell response against viral infection.

In summary, the presence of a complex sets of immune-related genes, alongside with the peculiar features of selected genes in Chinese giant salamander, highlights that this species is an attractive candidate to understand the immune systems of lower vertebrates. The genetic information presented in this study may lay a

foundation for in depth investigation of molecular mechanisms underlying antiviral immunity of this primitive amphibian.

Acknowledgements

This work was supported by the National Basic Research Program of China (2010CB126303), the Strategic Priority Research Program of Chinese Academy of Sciences (XDA08030202), the National Natural Science Foundation of China (31270213, 31202028, 31372551), and the Project of State Key Laboratory of Freshwater Ecology and Biotechnology (2011FBZ12).

Appendix A. Supplementary data

Supplementary data associated with this article can be found, in the online version, at http://dx.doi.org/10.1016/j.dci.2014.05.019.

References

Au, K.F., Sebastiano, V., Afshar, P.T., Durruthy, J.D., Lee, L.B., Williams, A., van Bakel, H., Schadt, E.E., Reijo-Pera, R.A., Underwood, J.G., Wong, W.H., 2013. Characterization of the human ESC transcriptome by hybrid sequencing. Proc. Natl. Acad. Sci. USA 110, E4821–4830.

Boudinot, P., Boubekeur, S., Benmansour, A., 2002. Primary structure and complementarity-determining region (CDR) 3 spectratyping of rainbow trout TCR beta transcripts identify ten V beta families with Vbeta6 displaying unusual CDR2 and differently spliced forms. J. Immunol. 169, 6244–6252.

Chen, G.C., Robert, J., 2011. Antiviral immunity in amphibians. Viruses 3, 2065–2086.

Chen, Z.Y., Gui, J.F., Gao, X.C., Pei, C., Hong, Y.J., Zhang, Q.Y., 2013. Genome architecture changes and major gene variations of *Andrias davidianus* ranavirus (ADRV). Vet. Res. 44, 101.

Cheriyath, V., Leaman, D.W., Borden, E.C., 2011. Emerging roles of FAM14 family members (G1P3/ISG 6–16 and ISG12/IFI27) in innate immunity and cancer. J. Interferon Cytokine Res. 31, 173–181.

Chinchar, V.G., Waltzek, T.B., 2014. Ranaviruses: not just for frogs. PLoS Pathog. 10, e1003850.

Conesa, A., Gotz, S., Garcia-Gomez, J.M., Terol, J., Talon, M., Robles, M., 2005. Blast2GO: a universal tool for annotation, visualization and analysis in functional genomics research. Bioinformatics 21, 3674–3676.

Danilova, N., Bussmann, J., Jekosch, K., Steiner, L.A., 2005. The immunoglobulin heavy-chain locus in zebrafish: identification and expression of a previously unknown isotype, immunoglobulin Z. Nat. Immunol. 6, 295–302.

Dong, W., Zhang, X., Yang, C., An, J., Qin, J., Song, F., Zeng, W., 2011. Iridovirus infection in Chinese giant salamanders, China. Emerg. Infect. Dis. 17, 2388–2389.

Edholm, E.S., Bengten, E., Wilson, M., 2011. Insights into the function of IgD. Dev. Comp. Immunol. 35, 1309–1416.

Gao, K.Q., Shubin, N.H., 2003. Earliest known crown-group salamanders. Nature 422, 424–428.

Geng, Y., Wang, K.Y., Zhou, Z.Y., Li, C.W., Wang, J., He, M., Yin, Z.Q., Lai, W.M., 2011. First report of a Ranavirus associated with morbidity and mortality in farmed Chinese giant salamanders (*Andrias davidianus*). J. Comp. Pathol. 145, 95–102.

Giallourakis, C.C., Benita, Y., Molinie, B., Cao, Z., Despo, O., Pratt, H.E., Zukerberg, L.R., Daly, M.J., Rioux, J.D., Xavier, R.J., 2013. Genome-wide analysis of immune system genes by expressed sequence Tag profiling. J. Immunol. 190, 5578–5587.

Gilchrist, M., Zorn, A.M., Voigt, J., Smith, J.C., Papalopulu, N., Amaya, E., 2004. Defining a large set of full length clones from a *Xenopus tropicalis* EST project. Dev. Biol. 271, 498–516.

Giudicelli, V., Lefranc, M.P., 1999. Ontology for immunogenetics: the IMGT-ONTOLOGY. Bioinformatics 15, 1047–1054.

Grayfer, L., De Jesús Andino, F., Robert, J., 2014. The amphibian (*Xenopus laevis*) type I interferon response to Frog Virus 3: new insight into ranavirus pathogenicity. J. Virol. 88, 5766–5777.

Humphrey, B.D., Calvert, C.C., Klasing, K.C., 2004. The ratio of full length IgY to truncated IgY in immune complexes affects macrophage phagocytosis and the acute phase response of mallard ducks (*Anas platyrhynchos*). Dev. Comp. Immunol. 28, 665–672.

Kiefer, F., Arnold, K., Künzli, M., Bordoli, L., Schwede, T., 2009. The SWISS-MODEL repository and associated resources. Nucleic Acids Res. 37, 387–392.

Lee, Y.H., Williams, A., Hong, C.S., You, Y., Senoo, M., Saint-Jeannet, J.P., 2013. Early development of the thymus in *Xenopus laevis*. Dev. Dyn. 242, 164–178.

Li, L., Wang, T., Sun, Y., Cheng, G., Yang, H., Wei, Z., Wang, P., Hu, X., Ren, L., Meng, Q., Zhang, R., Guo, Y., Hammarström, L., Li, N., Zhao, Y., 2012. Extensive diversification of IgD-, IgY-, and truncated IgY(ΔFc)-encoding genes in the red-eared turtle (*Trachemys scripta elegans*). J. Immunol. 189, 3995–4004.

Li, S., Lefranc, M.P., Miles, J.J., Alamyar, E., Giudicelli, V., Duroux, P., Freeman, J.D., Corbin, V.D.A., Scheerlinck, J.P., Frohman, M.A., Cameron, P.U., Plebanski, M., Loveland, B., Burrows, S.R., Papenfuss, A.T., Gowans, E.J., 2013. IMGT/HighV-QUEST paradigm for T cell receptor IMGT clonotype diversity and next generation repertoire immunoprofiling. Nat. Commun. 4, 2333.

Ma, J., Zeng, L., Zhou, Y., Jiang, N., Zhang, H., Fan, Y., Meng, Y., Xu, J., 2014. Ultrastructural morphogenesis of an Amphibian iridovirus isolated from Chinese giant salamander (*Andrias davidianus*). J. Comp. Pathol. 50, 325–331.

Magor, K.E., Higgins, D.A., Middleton, D.L., Warr, G.W., 1994. One gene encodes the heavy chains for three different forms of IgY in the duck. J. Immunol. 153, 5549–5555.

Marchalonis, J., Edelman, G.M., 1966. Phylogenetic origins of antibody structure. II. Immunoglobulins in the primary immune response of the bullfrog, *Rana catesbiana*. J. Exp. Med. 124, 901–913.

Meng, Y., Ma, J., Jiang, N., Zeng, L.B., Xiao, H.B., 2014. Pathological and microbiological findings from mortality of the Chinese giant salamander (*Andrias davidianus*). Arch. Virol. 159, 1403–1412.

Moriya, Y., Itoh, M., Okuda, S., Yoshizawa, A.C., Kanehisa, M., 2007. KAAS: an automatic genome annotation and pathway reconstruction server. Nucleic Acids Res. 35, 182–185.

Ohta, Y., Flajnik, M., 2006. IgD, like IgM, is a primordial immunoglobulin class perpetuated in most jawed vertebrates. Proc. Natl. Acad. Sci. USA 103, 10723–10728.

Ohta, Y., Goetz, W., Hossain, M.Z., Nonaka, M., Flajnik, M.F., 2006. Ancestral organization of the MHC revealed in the amphibian *Xenopus*. J. Immunol. 176, 3674–3685.

Parker, N., Porter, A.C., 2004. Identification of a novel gene family that includes the interferon-inducible human genes 6–16 and ISG12. BMC Genomics 5, 8.

Perera, J., Meng, L., Meng, F., Huang, H., 2013. Autoreactive thymic B cells are efficient antigen-presenting cells autoreactive thymic B cells are efficient antigen-presenting cells of cognate self-antigens for T cell negative selection. Proc. Natl. Acad. Sci. USA 110, 17011–17016.

Putta, S., Smith, J.J., Walker, J.A., Rondet, M., Weisrock, D.W., Monaghan, J., Samuels, A.K., Kump, K., King, D.C., Maness, N.J., Habermann, B., Tanaka, E., Bryant, S.V., Gardiner, D.M., Parichy, D.M., Voss, S.R., 2004. From biomedicine to natural history research: EST resources for ambystomatid salamanders. BMC Genomics 5, 54.

Ramirez-Gomez, F., Greene, W., Rego, K., Hansen, J.D., Costa, G., Kataria, P., Bromage, E.S., 2012. Discovery and characterization of secretory IgD in rainbow trout: secretory IgD is produced through a novel splicing mechanism. J. Immunol. 188, 1341–1349.

Robert, J., Cohen, N., 2011. The genus *Xenopus* as a multispecies model for evolutionary and comparative immunobiology of the 21st century. Dev. Comp. Immunol. 35, 916–923.

Ryazantsev, S., Tischenko, V., Nguyen, C., Abramov, V., Zav'yalov, V., 2013. Three-dimensional structure of the human myeloma IgG2. PLoS One 8, e64076.

Savan, R., Aman, A., Sato, K., Yamaguchi, R., Sakai, M., 2005. Discovery of a new class of immunoglobulin heavy chain from fugu. Eur. J. Immunol. 35, 3320–3331.

Tamura, K., Dudley, J., Nei, M., Kumar, S., 2007. MEGA4: molecular evolutionary genetics analysis (MEGA) software version 4.0. Mol. Biol. Evol. 24, 1596–1599.

Vogel, G., 1999. Frog is a prince of a new model organism. Science 285, 25.

Wang, T., Sun, Y., Shao, W., Cheng, G., Li, L., Cao, Z., Yang, Z., Zou, H., Zhang, W., Han, B., Hu, Y., Ren, L., Hu, X., Guo, Y., Fei, J., Hammarström, L., Li, N., Zhao, Y., 2012. Evidence of IgY subclass diversification in snakes: evolutionary implications. J. Immunol. 189, 3557–3565.

Wei, Z., Wu, Q., Ren, L., Hu, X., Guo, Y., Warr, G.W., Hammarström, L., Li, N., Zhao, Y., 2009. Expression of IgM, IgD, and IgY in a reptile, *Anolis carolinensis*. J. Immunol. 183, 3858–3864.

Ye, J., Fang, L., Zheng, H.K., Zhang, Y., Chen, J., Zhang, Z., Wang, J., Li, S., Li, R., Bolund, L., Wang, J., 2006. WEGO: a web tool for plotting GO annotations. Nucleic Acids Res. 34, 293–297.

Zhang, Q.Y., Gui, J.F., 2012. Atlas of Aquatic Viruses and Viral Diseases. Science Press, Beijing, pp. 251–253.

Zhao, Y., Pan-Hammarström, Q., Yu, S., Wertz, N., Zhang, X., Li, N., Butler, J.E., Hammarström, L., 2006. Identification of IgF, a hinge-region-containing Ig class, and IgD in *Xenopus tropicalis*. Proc. Natl. Acad. Sci. USA 103, 12087–12092.

Zhao, Y., Cui, H., Whittington, C.M., Wei, Z., Zhang, X., Zhang, Z., Yu, L., Ren, L., Hu, X., Zhang, Y., Hellman, L., Belov, K., Li, N., Hammarström, L., 2009. *Ornithorhynchus anatinus* (platypus) links the evolution of immunoglobulin genes in eutherian mammals and nonmammalian tetrapods. J. Immunol. 183, 3285–3293.

Zhu, R., Wang, J., Lei, X.Y., Gui, J.F., Zhang, Q.Y., 2013. Evidence for *Paralichthys olivaceus* IFITM1 antiviral effect by impeding viral entry into target cells. Fish Shellfish Immunol. 35, 918–926.

Zhu, R., Chen, Z.Y., Wang, J., Yuan, J.D., Liao, X.Y., Gui, J.F., Zhang, Q.Y., 2014. Extensive diversification of MHC in Chinese giant salamanders *Andrias davidianus* (AdMHC) reveals novel splice variants. Dev. Comp. Immunol. 42, 311–322.